Interaction Forces between Red Cells Agglutinated by Antibody. IV. Time and Force Dependence of Break-up

David F. J. Tees, Olivier Coenen, and Harry L. Goldsmith

McGill University Medical Clinic, Montreal General Hospital Research Institute, Montréal, Québec H3G 1A4, Canada

ABSTRACT   We report on an extension of a previously described method to measure the hydrodynamic force to separate doublets of fixed, sphered and swollen red cells cross-linked by antibody (S. P. Tha, J. Shuster, and H. L. Goldsmith. 1986. *Biophys. J.* 50:1117–1126). With a traveling microtube apparatus, doublets are tracked and videotaped in a slowly accelerating Poiseuille flow in 150-μm-diameter tubes, and the hydrodynamic normal force at break-up, F_n, is computed from the measured doublet velocity and radial position. Previous results showed a large range of F_n, the mean of which increased with [antiserum], and an absence of clustering at discrete values of F_n. Since it was assumed that the cells separate the instant a critical force to break all crossbridges was reached, lack of clustering could have been due to the use of a polyclonal antiserum. We therefore studied the effect of monoclonal IgM or IgA antibody on the distribution of F_n. The results showed that the data are as scattered as ever, with F_n varying from 2 to 200 pN, and exhibit no evidence of clustering. However, the scatter in F_n could be due to the stochastic nature of intercellular bonds (E. Evans, D. Berk, and A. Leung. 1991a. *Biophys. J.* 59:838–848). We therefore studied the force dependence of the time to break-up under constant shear stress (F_n from 30 to 200 pN), both in Poiseuille and Couette flow, the latter by using a counter-rotating cone and plate rheoscope. When 280 doublets were rapidly accelerated in the traveling microtube and then allowed to coast in steady flow for up to 180 s, 91% survived into the constant force region; 16% of these broke up after time intervals, t_P, of 2–30 s. Of 340 doublets immediately exposed to constant shear in the rheoscope, 37% broke after time intervals, t_C, from <1 to 10 s. Thus, doublets do indeed break up under a constant shear stress, if given time. The average time to break-up decreased significantly with increasing force, while the fraction of doublets broken up increased. At a given F_n, the fraction of break-ups decreased with increasing [IgM], suggesting that the average number of bonds had also increased. Using a stochastic model of break-up (G. I. Bell. 1978. *Science (Washington DC)*. 200:618–627; E. Evans, D. Berk, and A. Leung. 1991. *Biophys. J.* 59:838–848) and a Poisson distribution for the number of bonds, N_b, break-up in slowly accelerating Poiseuille flow and in immediate shear application in Couette flow was simulated. In Poiseuille flow, the observed range and scatter in F_n could be reproduced assuming $\langle N_b \rangle > 5$. In the rheoscope, the time intervals and number of rotations to break-up, t_C, were quite well reproduced assuming $\langle N_b \rangle = 4$. The similarity of $\langle F_n \rangle$ for monoclonal IgM and IgA for doublet break-up under constant slow acceleration is compatible with the conclusion of Evans et al. (1991a) for normal red cells and Xia et al. (manuscript submitted for publication) for sphered and swollen red cells, that the applied force extracts the antigen from the cell membrane.

GLOSSARY

Nomenclature

b	sphere radius		P_b	probability of break-up in time Δt, defined by Eq. 16
c	parameter in stochastic model of break-up (Evans et al., 1991a)		r	antibody-antigen separation distance
			r_o	width of free energy minimum (Bell, 1978)
C	orbit constant defined in Eq. 5		r_e	equivalent spheroidal axis ratio of a doublet, defined by Eq. 4
E_o	depth of bond free energy minimum (Bell, 1978)			
f	force per bond		R	radial distance from tube axis
f_c	critical force per bond for instantaneous break-up		R_o	tube radius
F_n, F_s	hydrodynamic normal and shear forces, respectively (given by Eqs. 7 and 8)		t_o	parameter in stochastic model of break-up (Evans et al., 1991a)
G	shear rate		t_C, t_P	respective times to break-up in Couette and Poiseuille flow
$G(R)$	shear rate at radial distance R from the tube axis in Poiseuille flow		t_b	time to break-up in stochastic model
k	Boltzmann constant		T	period of rotation
l_1	projection of doublet major axis along the X_1 axis		T_K	absolute temperature
l_{13}, l_{23}	projections in the X_1X_3- and X_2X_3-planes		u_1, u_2, u_3	components of undisturbed fluid velocity along X_i, $i = 1, 2, 3$
n	number of doublets			
N	number of rotations in time τ		$u_3(R)$	component of fluid velocity along X_3 at radial distance R from tube axis, in Poiseuille flow
N_s	number of steps during one rotation			
N_b	number of bonds		X_1, X_2, X_3	Cartesian coordinates
			$\Delta X_2(R)$	cone and plate separation distance at radial distance R from center

Greek Symbols

η	suspending fluid viscosity

θ_1, θ_2	polar angles of doublet major axis with respect to X_1 and X_2 as polar axes
κ	antigen-antibody reverse reaction rate constant
τ	time to execute N rotations
τ_o	reciprocal of natural frequency of oscillation of atoms in solids (Bell, 1978)
ϕ_1, ϕ_2	azimuthal angles of doublet major axis with respect to X_1 and X_2 as polar axes
ψ	cone angle
Ω_c, Ω_p	respective angular velocities of cone and plate

INTRODUCTION

Measurement of the physical strength of the bonds linking biological cells to each other and to surfaces is an important prerequisite for the characterization of adhesion processes occurring in the circulation and elsewhere, such as cancer metastasis, platelet thrombosis, and leukocyte margination and extravasation. In the case of cell surface adhesion, a number of models (Dembo et al., 1988; Cozens-Roberts et al., 1990a; Hammer and Apte, 1992) have recently been proposed and used to predict the effect of fluid shear stress on such parameters as the number of adherent cells remaining on the surface, the force required to detach adherent cells, and their rolling velocity at surfaces in flow. Techniques for measuring these parameters have also been described (Cozens-Roberts et al., 1990b; Lawrence and Springer, 1991; Tözeren et al., 1992; Xia et al., 1989). In the case of cell-cell adhesion, attention has focused on the forces required to separate bound aggregates. Bell (1978) developed a model, based on the theory of the strength of materials, to describe the strength of bonds and the kinetics of their formation and breakage. This and other models have since been developed further (Bell et al., 1984; Evans, 1985; Tözeren, 1990). Measurements of the force of adhesion between cells, however, have been attempted by relatively few workers. Bongrand et al. (1979) used the known shear field to calculate the average force on a suspension of erythrocytes forced through a calibrated syringe needle. This method has been used by Capo et al. (1982) for a quantitative study of thymocyte aggregation. Evans et al. have pioneered the double micropipette aspiration technique to measure forces required to separate cell doublets (Evans and Leung, 1984; Sung et al., 1986). Separation forces have been obtained for both "point" contacts (Evans et al., 1991a) and for large contact areas (Evans et al., 1991b; Berk and Evans, 1991). This method allows individual adherent cell doublets to be examined and hence can be used to study cell adhesion forces in detail instead of measuring average properties. Detailed study of doublets of red blood cells agglutinated with a monoclonal antibody to an integral membrane protein, a polyclonal antibody and a lectin, both specific to the blood group A antigen, showed that the forces were all approximately the same (10–20 pico-newtons = 1–2 μdyne). This was interpreted as being due to the extraction of the receptor from the cell membrane in all three cases, a hypothesis that was confirmed using fluorescence transfer studies. It was also found that doublets held under a constant force sometimes broke up after time lags of as much as 30 s.

The present paper is concerned with the extension of a previously described method for measuring the force required to detach freely suspended adherent cell pairs subjected to shear flow. In this technique, the hydrodynamic force necessary to separate doublets of sphered swollen red blood cells (SSRC) agglutinated with antibodies to the blood group B antigen is obtained by observing doublet break-up in an accelerating Poiseuille flow using a traveling microtube apparatus. Equations were derived for the forces acting on a doublet of equal-sized rigid spheres in a linear shear field (Tha and Goldsmith, 1986) and used to estimate the force of adhesion of SSRC doublets agglutinated with a polyclonal antibody to the blood group B antigen (Tha et al., 1986). A micropipette aspiration technique was also used to compare the force of separation with that obtained in shear flow (Tha and Goldsmith, 1988). Measurements of the forces at break-up of a large number of SSRC doublets failed to show clustering around a set of discrete force levels corresponding to different numbers of antigen-antibody cross-bridges. Since a polyclonal antibody was used, the fact that no such clustering was seen could be explained as being due to different forces of attachment for the different antibodies within the antiserum to the same antigen. Combinations of the different cross-linking antibodies would explain the scattered break-up forces. To eliminate this problem, the obvious next step was to use a *monoclonal* antibody to the same antigen. Results reported below show that the data are as scattered as ever, with no evidence of clustering.

Hitherto, our work on doublet break-up has assumed that there is no time lag between a threshold force (the force required to break n bonds) being reached and doublet separation. The observation of a range of break-up times for red cell doublets held under a constant force by Evans et al. (1991a), however, suggests that doublet break-up is a random event, the probability of which varies with the magnitude and duration of applied force. This has serious implications for the forces of separation at break-up reported in our previous experiments in steadily accelerating flow, since a doublet might well have broken up at a separation force lower than that measured at break-up, had the particle been given more time under the lower force. Since break-up under force seems to be a random event, the force measured at break-up will overestimate the minimum force of attachment by a random amount. This would explain why the data show no clustering.

If bonds are properly characterized by a force-dependent lifetime, then an attempt to identify a clearly defined force per bond is not appropriate. A more useful procedure would be to measure the force dependence of the average time for bond break-up. This requires the observation of doublets at predetermined forces until break-up. Accordingly, we present experimental work on the characterization of the anti-B antibody–B-antigen bond in terms of the time to break-up under applied stress. Experiments using both rapid acceleration to a predetermined shear rate in Poiseuille flow and virtually instantaneous acceleration to a predetermined shear rate in Couette flow have been carried out.

THEORY

Rotations of doublets of spheres in shear flow

We consider a doublet of equal-sized rigidly linked spheres of radius b suspended in a liquid of viscosity η with the particle center of rotation at the origin of a linear shear field,

$$u_1 = 0, \qquad u_2 = 0, \qquad u_3 = GX_2, \qquad (1)$$

where u_i are the components of the undisturbed flow along the coordinates, X_i, of the shear field and G is the shear rate. As shown in Fig. 1, the orientation of the axis of revolution or major axis of the doublet (Fig. 1, arrows) is described by θ_1 and ϕ_1, the respective polar and azimuthal angles with respect to X_1, the polar and vorticity axis, as well as by θ_2 and ϕ_2, with respect to X_2, the polar axis, and the transformation equations

$$\tan \phi_2 = \tan \theta_1 \sin \phi_1 \qquad (2a)$$

$$\cos \theta_1 = \sin \theta_1 \cos \phi_1. \qquad (2b)$$

The doublet rotates with periodically varying angular velocity given by

$$\frac{d\phi_1}{dt} = \frac{G}{r_e^2 + 1}(r_e^2 \cos^2\phi_1 + \sin^2\phi_1), \qquad (3)$$

with a period of rotation (Goldsmith and Mason, 1967), T:

$$T = \frac{2\pi}{G}\left(r_e + \frac{1}{r_e}\right), \qquad (4)$$

where r_e, the axis ratio of the equivalent ellipsoid for a doublet of touching rigid spheres (Wakiya, 1971) equals 1.98. The predicted dimensionless period of rotation, TG, is therefore = 15.61, a value confirmed by experiment (Tha et al., 1986). The equation relating θ_1 to ϕ_1 in each orbit is (Goldsmith and Mason, 1967)

$$\tan \theta_1 = \frac{Cr_e}{(r_e^2 \cos^2\phi_1 + \sin^2\phi_1)^{1/2}}, \qquad (5)$$

the equation of a spherical ellipse the eccentricity of which is defined by the orbit constant C. This constant may take on values between the limits 0 ($\theta_1 = 0°$ at all ϕ_1), when the doublet is aligned with and spins about the vorticity axis, and ∞ ($\theta_1 = 90°$ at all ϕ_1), when the doublet rotates in the X_2X_3-plane without axial spin. Diagrams of doublet orientation for $C = \infty$ and $C = 1.0$, when observed along the X_1- and X_2-axes, are shown in Fig. 1.

In the experiments carried out in the traveling microtube (Poiseuille flow), doublets were observed along the X_1-axis, normal to the median, diametrical plane of the tube. The particle is seen projected onto the X_2X_3-plane with the axis of revolution having length $l_{23} = 2b \sin \theta_1$. As shown in Fig. 1, when $C = \infty$, $\theta_1 = 90°$, $l_{23} = 2b$ at all ϕ_1. For $C < \infty$, $l_{23} < 2b$ and the projection of the doublet appears foreshortened, the projected length varying with ϕ_1.

In the experiments carried out in the rheoscope (Couette flow), doublets were observed along the X_2-axis. The particle
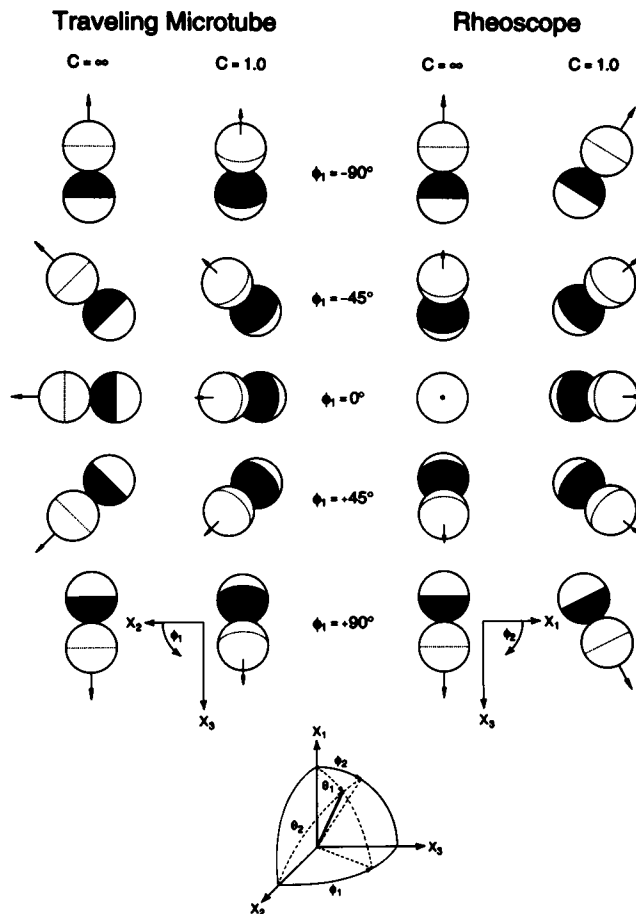

FIGURE 1 The orientations of a doublet of rigid spheres over one half-orbit, as observed with the SSRC in the traveling microtube and the rheoscope. Doublet rotation is defined by the Cartesian (X_1, X_2, X_3) and spherical polar (ϕ_1, ϕ_2; θ_1, θ_2) coordinates constructed at the doublet center of rotation. The orientations were calculated using Eq. 5 for orbit constants $C = \infty$ and 1.0. The arrows indicate the direction of doublet major axis (heavy line in the coordinate diagram). Doublets in Poiseuille flow were observed in the X_2X_3 (median) plane of the tube along the X_1 (vorticity) axis. Doublets in Couette flow were observed in the X_1X_3-plane along the X_2-axis. When $C = \infty$, $\theta_1 = 90°$ at all ϕ_1, the doublet axis rotates in the X_2X_3-plane. Therefore, when viewed in the median plane of the microtube there is no foreshortening of the doublet axis, whereas when viewed in the rheoscope in the X_1X_3-plane, the particles are seen tumbling end over end. When $C = 1.0$, the doublet axis rotates with variable $\theta_1 < 90°$, a minimum (45°) at $\phi_1 = 0°$ and a maximum (60°) at $\phi_1 = \pm90°$. Therefore, when viewed in the X_2X_3-plane, the doublet axis is foreshortened with l_{23} a minimum at $\phi_1 = 0°$, whereas when viewed in the X_1X_3-plane, the doublet is seen rocking to and fro between $\phi_{2max} = \pm60°$.

is seen projected onto the X_1X_3-plane with the major axis having length

$$l_{13} = 2b \sin \theta_2 = 2b(1 - \sin^2\theta_1\cos^2\phi_1)^{1/2}. \qquad (6)$$

Here, when $C = \infty$, $\phi_2 = 90°$ at all ϕ_1, and $l_{13} = 0$ and $2b$ at $\phi_1 = 0°$ and $90°$, respectively. Thus, as illustrated in Fig. 1, the doublet is seen to tumble end over end, one cell completely obstructing the view of the other at $\phi_1 = 0°$; when $\phi_1 \neq 0$, the projection of the major axis in the X_1X_3-plane is aligned with the X_3-axis, the direction of flow. When $C < \infty$, the doublet axis appears to rock back and forth between $\phi_{2max} = \theta_{1max}$ (Eq. 2, $\phi_1 = +90°$) and $\phi_{2min} = \theta_{1max}$

($\phi_1 = -90°$), at which points the doublet lies in the X_1X_3-plane, and $l_{13} = 2b$ is a maximum.

Forces on doublets in shear flow

The normal force, F_n, acting along, and shear force, F_s, acting normal to the doublet major axis, have been computed (Tha and Goldsmith, 1986) and are given by

$$F_n = 19.33\eta Gb^2 \sin^2\theta_1 \sin 2\phi_1, \tag{7}$$

$$F_s = 7.02\eta Gb^2 \sin \theta_1$$

$$\times \left\{ \frac{(2\sin^2\theta_1\cos^2\phi_1 - 1)^2\sin^2\phi_1 + \cos^2\theta_1\cos^2\phi_1}{1 - \sin^2\theta_1\cos^2\phi_1} \right\}^{1/2}. \tag{8}$$

Although the above treatment applies strictly to a linear shear field, Eqs. 3–5, 7, and 8 have been shown to apply in Poiseuille flow provided the velocity gradient can be considered constant over the radial distance occupied by the particle (<7% of the tube diameter in the present work).

Since the angular velocity of the doublet varies periodically in each orbit, both normal and shear forces vary periodically in each orbit. The normal force is alternately compressive and tensile in successive quadrants of each half-orbit, and the shear force (which must equal the force due to fluid mechanical torques on the spheres of the doublet in order for there to be no net torque about the center of the doublet axis; Tha and Goldsmith, 1986) alternates between zero and maximum values in each quadrant. When rotating in a $C = \infty$ orbit, the angle factors (trigonometric functions) in Eqs. 7 and 8 reduce to sin $2\phi_1$ and cos $2\phi_1$, respectively. Therefore, the maximum tensile force occurs at $\phi_1 = 45°$ and the maximum shear force at $\phi_1 = 0$ and $90°$. When rotating in orbits having $C < \infty$, the maxima in the forces (i.e., the maxima in the angle factors) occur at different ϕ_1, depending on the value of C (e.g., for $C = 0.5$, the maximum occurs at $\phi_1 = 60°$). The ratio of the maximum F_3 to maximum F_s is just the ratio of their coefficients, 2.75 (Tha and Goldsmith, 1986).

The time, Δt, in a given orbit required for a doublet to rotate from ϕ_1 to ($\phi_1 + \Delta\phi_1$) is, from Eq. 3, inversely proportional to the shear rate, G:

$$\Delta t = \frac{r_e + 1/r_e}{G} \left| \tan^{-1}\frac{1}{r_e}\tan \phi_1 \right|_{\phi_1}^{\phi_1 + \Delta\phi_1}. \tag{9}$$

In a given time, τ, the number of orbits, N, executed by the doublet increases with G:

$$N = \frac{\tau}{T} = \frac{\tau G}{2\pi(r_e + 1/r_e)}. \tag{10}$$

Therefore, the total time for which the normal and shear forces (Eqs. 7 and 8) act during rotation in the interval $\Delta\phi_1$ during τ is given by

$$N\Delta t = \frac{\tau}{2\pi} \left| \tan^{-1}\frac{1}{r_e}\tan \phi_1 \right|_{\phi_1}^{\phi_1 + \Delta\phi_1}, \tag{11}$$

which is independent of G, since the increase in N is com-

pensated by the decrease in time, Δt, required to rotate through $\Delta\phi_1$. Thus, while the magnitude of the hydrodynamic force is directly proportional to the shear rate, the duration of exposure of the doublet to this force in a given time is independent of shear rate. It should be emphasized, however, that with increasing G and increasing angular velocity, the corresponding increase in $dF_{n,s}/dt$ may have profound effects on the rate and extent of doublet bond breakage.

MATERIALS AND METHODS

Preparation of sphered swollen red blood cells

Rigid spherical red blood cells were prepared as previously described (Tha et al., 1986). Briefly, type B blood was drawn from healthy volunteers into tubes containing EDTA and washed six times in isotonic phosphate buffer (containing 1 mM Mg^{2+}) to remove plasma and buffy coat. Packed red cells were simultaneously sphered and swollen in a solution containing 66 μM sodium dodecyl sulfate and 200 mM glycerol and then fixed after 15 s with electron microscope pure glutaraldehyde at a final concentration of 0.085%. The resulting fixed cells were washed six times with filtered saline and then incubated for 1 h in 0.46 M lysine to bind any remaining unreacted aldehyde. After fixation, the cells were stable to aggregation (less than 0.2% were aggregated by the process) and did not change shape or volume in distilled water or concentrated sucrose solutions. Scanning electron microscopy showed the cells to be of high sphericity with some small surface asperities. The mean cell diameter, determined by videotape analysis of a population of 316 cells, was 6.42 ± 0.31 μm.

The sphered, swollen cells were suspended in 46–56% sucrose in phosphate buffer, depending on the desired viscosity (from 8.4 to 25.1 mPa·s at 25°C), at concentrations of 1.25 or 2.5 × 10^4 cells/μl. Monoclonal antiblood group B, affinity-purified IgM antibody (DAKO Corporation, Dimension Labs, Mississauga, ON, Canada) was added at final concentrations of 0.075–0.60 nM. The suspensions were incubated overnight at room temperature while stirred on a rotary mixer at 12 rpm.

In addition to the IgM series, a monoclonal anti-B IgA antibody (E_2 83-52, a generous gift of Dr. M. Herlyn, Wistar Institute, Philadelphia) was used for some experiments at a concentration of 0.15 nM. These IgA experiments allowed a decavalent molecule to be compared with a divalent one.

An estimate of the upper limit on the number of cross-bridges between SSRC doublets can be made from the concentration of antibody. In a suspension containing 0.3 nM antibody and 2.5 × 10^4 SSRC/μl, an average of 7500 molecules of antibody are available for binding to each cell. The mean surface area of the SSRC is 129 μm^2, and assuming that bonding occurs at surface separations between 20 and 45 nm, the maximum area for SSRC cross-linking by IgM is estimated (Tha and Goldsmith, 1986) to be ~0.25 μm^2. Since the red cell has ~10^6 blood group B antigen sites on its surface (Economidou et al., 1967), there should be ~2000 sites in the ~0.25 μm^2 contact area on each cell. If every antibody molecule in the suspension were bound to an antigenic site, and surface coverage were uniform, the average number of antibodies in the region of cross-linking would be ~15 on each of the cells of a doublet (making a maximum possible 30 bonding molecules). Since many of the antibody molecules in the region of binding will not participate in the cross-linking and some of the antibody in the suspension will not be adsorbed, this number is probably an overestimate. Consequently, the number of cross-bridges linking the SSRCs is small and may be as low as one in some cases.

Flow Systems

Poiseuille flow

In the experiments described below, cell suspensions were subjected to laminar viscous flow through a 150-μm-diameter glass tube using gravity feed between infusion and collecting reservoirs. The tube lay on a microscope slide and was enclosed in a chamber filled with suspending fluid to

minimize optical distortion. The slide and reservoirs were mounted on a jig and attached to the vertically sliding platform of a hydraulically driven traveling microtube apparatus, details of which have previously been given (Vadas et al., 1973; Tha et al., 1986).

As previously described (Takamura et al., 1979; Tha et al., 1986), doublets of SSRC were viewed with a videocamera (model C1000; Hamamatsu Systems, Inc., Waltham, MA) attached to a horizontally positioned microscope at 500× to 650× magnification and tracked by moving the platform upward at a velocity equal to that of the downward-flowing particles. Simultaneously, another videocamera (model AVC 3260S; Sony Canada, Ltd., Montreal, PQ, Canada) was trained on an odometer, recording the axial distance traveled by the microtube. Images from these two cameras were combined into a single frame using a screen splitter (Thalner Electronics, Ann Arbor, MI). A digital time display was added to the image by a time-date generator (Panasonic model WJ-810; Matsushita Electric of Canada, Ltd., Mississauga, ON, Canada), and the resulting video sequence was recorded on videotape at 30 frames s^{-1} by a video cassette recorder (Panasonic model AG-7300; Matsushita) and displayed on a 15-inch monitor (model V19-121; Electrohome, Ltd., Kitchener, ON, Canada). Measurements of SSRC size, orientation, and position were made on the monitor using a superimposed videoposition analyzer (model VPA-1000; FOR-A Co., Ltd., Tokyo, Japan) calibrated with a micrometer scale.

The shear rate in Poiseuille flow at a radial distance R from the axis of the microtube of radius R_0 was calculated from the doublet linear velocity, $u_3(R)$, using the equation

$$G(R) = \frac{2u_3(R)R}{R_0^2 - R^2} \qquad (12)$$

since it has been shown that, provided $b/R_0 \ll 1$, the doublet velocity at R is equal to that of the undisturbed fluid at this radial position (Goldsmith and Mason, 1962).

Couette flow

The immediate shear application experiments were carried out using a transparent, counter-rotating cone and plate rheoscope system (model MR-1; Myrenne Instruments, Fremont, CA) having a nominal cone angle of 2° and rotational velocities, identical for cone and plate, adjustable from 0.87 to 42 rpm. The rheoscope replaced the stage of a Leitz Diavert inverted microscope (Ernst Leitz, Ltd., Midland, ON, Canada). The midplane of the cone and plate gap was observed with a 20× objective at radial distances of 600 to 800 μm from the center of rotation. Observations were made using a CCD video camera with an electronic shutter set for 1 ms (model AVC-D7; Sony) to avoid blurring of doublets at high particle angular velocities. The resulting video images were then passed to the recording and display electronics described in the Poiseuille flow section above.

For the cone and plate geometry, the shear rate at a radial distance R from the cone center is given by

$$G(R) = \frac{(\Omega_c - \Omega_p)R}{\Delta X_2(R)}, \qquad (13)$$

where Ω_c and Ω_p are the respective angular velocities of cone and plate and $\Delta X_2(R) = R \tan \psi$ is the gap width between them, ψ being the cone angle. Therefore, at all R,

$$G = \frac{\Omega_c - \Omega_p}{\tan \psi}. \qquad (14)$$

The rheoscope cone and plate angular velocities are adjusted using a 10-turn variable resistor, the setting of which was linearly related to Ω_c and Ω_p. The cone angle was verified using a Starrett digital gauge with cartridge-type gauging head (no. 812-13; L. S. Starrett Co., Athol, MA) to measure the gap width between the cone and plate surfaces at different radial distances. The cone angle was found to be 2.0 ± 0.1° by linear least-squares analysis.

As a further check on the cone angle, the periods of rotation of 25 doublets at various R were measured at the lowest steady shear rate pos-

sible (5.4 s^{-1}), and TG was computed using values of G from Eq. 14 for $\psi = 2°$. At $R \geq 600$ μm (corresponding to $\Delta X_2 \geq 21$ μm), a mean value for TG of 15.4 ± 0.5 was found, in good agreement with that predicted by theory (Wakiya, 1971), 15.61, and with that previously found in Poiseuille flow (Tha et al., 1986), 15.5 ± 0.3. The TG values increased to >18 at $R = 400$ μm. At this radial distance, where ΔX_2 (≤ 14 μm) is barely larger than the doublet length, the increase in TG is likely due to a wall effect (Goldman et al., 1967), as previously documented for doublets rotating close to the tube wall in Poiseuille flow (Tha et al., 1986). Consequently, observations of doublet break-up in Couette flow were made at radial distances of ≥ 600 μm.

Since $\Omega_c = -\Omega_p$, a layer of zero translational velocity was located in the midplane at the origin of the field of Couette flow, in which layer doublets could be viewed indefinitely. Most doublets, however, were observed close to, but not in, the midplane and thus drifted slowly across the field of view.

Data acquisition

Normal force determination in Couette and Poiseuille flow

It is not known whether normal or shear forces play the principal role in bringing about the separation of the cells of the doublet. Whether the shear or normal force is responsible for doublet separation is moot, however. As suggested by Bell (1978), inasmuch as the antibodies are free to orient themselves relative to the sphere surface, the shear force at the contact may be turned into stresses on the bonds that are tensile. Since the maximum normal force is about 2.5 times the maximum shear force, it is reasonable to concentrate on the former. Here, the results are given in terms of the normal force acting on a doublet at break-up, computed using Eq. 7 with the experimentally determined values of η, G, b, and θ_1.

Since it is not possible to determine by inspection the orientation at which the members of a doublet separate, beyond the observation that it takes place in the last quarter orbit, $0° < \phi_1 < 90°$, it is not possible to compute the force at the moment of break-up. Instead, as in the previous work, it is assumed that break-up occurred at the point in the final half-orbit where F_n is a maximum. Consequently, the angle θ_1 was measured, and the angle ϕ_1 that maximizes $\sin^2 \theta_1 \sin 2\phi_1$, the angle factor in Eq. 7, was found.

The viscosity of a sample of the suspending medium was measured in a thermostated Cannon-Ubbelohde capillary viscometer at 21, 24, and 27°C. The temperature shown on a digital thermometer placed on the microtube glass slide, or the rheoscope housing, was recorded after each break-up, and the viscosity was derived by interpolation.

From the videotape recording of break-up in the microtube experiments, eight position analyzer measurements of the SSRC diameter, $2b$, the radial distance from the tube wall ($R_0 - R$), and the projected length, l_{23}, of the doublet major axis in the X_2X_3-plane at $\phi_1 = 0°$, were made and averaged. The linear velocity of the doublet, $u_3(R)$, was determined using frame-by-frame playback of the recorded doublet motion, and the shear rate, $G(R)$, was then calculated using Eq. 12. The orbit constant, C, was computed from Eq. 5, using θ_1 obtained from l_{23}. This enabled the maximum value of F_n to be computed.

In the rheoscope experiments, the position analyzer was used to make eight measurements of $2b$ and the projection of the doublet major axis on the X_1-axis at $\phi_1 = 90°$, $l_1 = 2b \cos \theta_1$ (Fig. 1), which were then averaged and used to compute θ_1 and C (using Eq. 5). The shear rate, G, was computed from Eq. 4 using the mean value of the period of rotation, T, measured over 10–20 orbits depending on the time of observation of the doublet. If the doublet broke up in the first rotation, G was calculated using Eq. 14 with $\psi = 2.0°$ and $\Omega_c = -\Omega_p$ determined from the previously calibrated variable resistor setting.

Constant slow acceleration in Poiseuille flow

As in the original experiments of Tha et al. (Tha et al., 1986), after a doublet had been identified in slow steady flow ($u_3(0) \approx 5$ μm s^{-1}), the flow rate was accelerated by continuously pumping silicone oil from a Harvard pump into the infusion reservoir on top of the cell suspension. The oil infusion rate was adjusted to produce a linear acceleration of 25 μm·s^{-2} at the tube axis.

Doublets were tracked in steadily accelerating flow until either they broke up or the maximum tracking speed of the traveling microtube drive (1 mm·s^{-1}) was reached, in which case the doublet was lost.

Halted rapid acceleration in Poiseuille flow

To determine whether doublets subjected to a constant shear stress, $G(R)\eta$, in each rotational orbit break up after a noticeable time lag, experiments were performed in which silicone oil was pumped into the infusion reservoir at a high flow rate for a short time, resulting in a rapid linear acceleration of ~150 μm·s^{-2} at the tube axis. After infusing for 5 to 15 s, depending on the desired magnitude of the force and the doublet radial distance from the tube axis, infusion was suddenly halted (acceleration ceased within 1 s of turning off the infusion pump), and the particle was tracked under steady flow conditions. The time to break-up, t_P, in steady flow was recorded.

To determine the infusion time necessary to attain a given force, a doublet, once selected, was halted with its major axis at $\phi_1 = 0°$. Measurements of $2b$, $R_o - R$, and l_{23} were made, and, along with the known viscosity, were entered into a microcomputer in order to calculate $G(R)$ and hence the $u_3(R)$ necessary for a given value of F_n. The computer was programmed with the known relation between infusion rate and $u_3(0)$ in the tube to signal the observer when the desired value of $u_3(R)$ was reached, at which time the infusion pump was turned off. The doublet then traveled with steady translational velocity until it either broke up or was lost at the lower end of the microtube. The available tracking distance of 3.5–4.0 cm allowed doublets to be observed for 1 to 3 min after the start of steady flow. The steady velocity reached varied within 20% of that desired, due to errors in the measurement of $2b$, $R_o - R$, and l_{23}, as well as to changes in the relation between infusion rate and doublet acceleration due to variations in the infusion rate with temperature.

Although doublet linear velocity should have been constant after halting oil infusion (to within the experimental error of ±2%), this was true in only 33% of particles studied. In 45% of the doublets, $u_3(R)$ increased, and in 12% it decreased steadily by 2–10% before break-up or loss at the end of the tube. In the remaining 9% of doublets, $u_3(R)$ changed by more than 10%, due mostly to collisions with other cells leading to significant radial displacement of the doublet center of rotation. If such an increase or decrease occurred, the force on the doublet was calculated using the last value of $u_3(R)$ before either break-up or loss at the end of the tube.

About one-half of all observed break-ups were not analyzed because the separation was apparently caused by an interaction between the doublet under observation and another single cell or doublet. Such interactions may have induced break-up through an increase in the hydrodynamic force acting on the particle, either by increasing the orbit constant, C, or by radially displacing the doublet toward the tube wall and a higher shear rate. A few interactions appeared to involve the transient attachment of an interacting single cell or doublet with one of the members of the doublet. The formation of the resulting triplet or quadruplet may have imposed an additional hydrodynamic force on the doublet cross-bridges, which in some cases led to break-up, one or two rotational orbits after the interaction occurred.

In order to reduce the likelihood of such collisions between doublets and other particles during the longer observation times in the halted acceleration experiments, the SSRC concentration was halved from that used in the constant acceleration experiments, to 1.25×10^4 cells/μl. The antibody concentration was also halved to preserve the ratio of the number of antibody molecules to the number of SSRC. The two antibody concentrations used were therefore 0.075 and 0.150 nM.

Couette flow

For the immediate shear application experiments, 100 μl of SSRC suspension containing 1.25×10^4 cells/μl and 0.075 or 0.150 nM antibody, was pipetted into the rheoscope. Doublets were allowed to form as a result of two-body collisions at the lowest $G = 5.4$ s^{-1} (corresponding to $F_{n, max} \approx 16$ pN, for $C = \infty$ and $\eta = 15$ mPa·s) and observed at 250× magnification. Once a doublet was spotted, flow was stopped, the magnification was increased to 320× and the doublet rotation was recorded on videotape at $G = 5.4$ s^{-1}. Flow was again stopped while the sphere diameter and the

projected length, l_1, were measured and entered, along with the known viscosity, into a microcomputer to determine the rheoscope variable resistor speed setting required to produce a desired force. With the magnification back to 250× to increase the field of view, the doublet was observed visually through the microscope, where an even larger field of view was available, and allowed to execute several rotations at the lowest G to verify that it had not broken up while the above measurements were being made. Break-up at zero or very low G occurred in ~20% of doublets in the Couette experiments and was occasionally also observed in the microtube. The rheoscope was then set in motion at the required speed dial setting, the desired shear rate being reached within 60 ms (two videotape frames). The doublet was observed and recorded on videotape until it either broke up or was lost from the field of view. If break-up was recorded in the videocamera field of view, the time to break-up from the start of flow, t_C, could be measured to within two to three video frames (±0.1 s). If break-up was observed visually, outside the video camera field of view, the time of break-up was signaled by stopping the rheoscope motion. In this case, the error in t_C was estimated to be a reaction time, +0.2 s.

Since it was difficult to make accurate measurements of the doublet diameter and orientation during flow at high G, the force acting on the doublet was computed using the values of $2b$ and l_1 measured at low G and 320× magnification. This assumed that the orbit constant did not change significantly before the doublets broke up or were lost to view.

As with the halted acceleration experiments in Poiseuille flow, described above, about 25% of the break-ups observed were not included in the analysis, since the presence of other cells close to the doublet near the time of break-up suggested that they might have been the cause.

Error analysis

Viscosity. Temperature fluctuations of ±0.1°C over the course of a doublet tracking account for an error of ±0.1 mPa·s, <1% of the viscosity of most sucrose suspending media used.

Doublet diameter. The SD of the eight position analyzer measurements normally made of the SSRC diameter, $2b$, was typically one position analyzer division representing an error of ±6%.

Angle factors. Here, errors arise from uncertainty in the computation of the orbit constant, C, which in turn depends on errors in the measured length of the projected doublet axis, l_{23} in Poiseuille flow and l_1 in Couette flow. In Poiseuille flow, these errors increased from 2.5 to 5%, as C decreased from 10 to 1.0, respectively, but decreased from 5 to 2.5% in Couette flow. For values of $C > 10$, when θ_1 is close to 90° throughout the orbit, the above errors lead to very small differences in the maximum value of the angle factor. Calculations show that the maximum error was approximately ±3%.

Shear rate. In Poiseuille flow, the error in $G(R)$ depends on the uncertainty in the final measured $u_3(R)$, taken to be about ±5%, and in the measurement of radial distance from the tube wall, estimated to be ±1%. In Couette flow, the error in G depends on the uncertainty in measuring the period of rotation, T (Eq. 4). Since the doublets were observed over 5–20 orbits, over a period of 2–5 s, and the number of orbits was determined to within one videotape frame (0.03 s), the error in T, and hence G, was negligible. In cases where the doublet broke up within one rotation, Eq. 14 was used to calculate G; here, the uncertainty in the rheoscope speed dial setting used to compute G was ±1%.

The above errors were propagated through the force calculations for individual break-ups. Using standard formulae for independent errors (Bevington, 1969), calculations show that the total error in the computed forces varied from ±5 to ±15%.

RESULTS

Poiseuille flow: continuous slow acceleration

A scatter plot of the maximum normal force, F_n, at break-up in the constant slow acceleration experiments at IgM concentrations of 0.15, 0.30, and 0.60 nM is shown in Fig. 2 a.
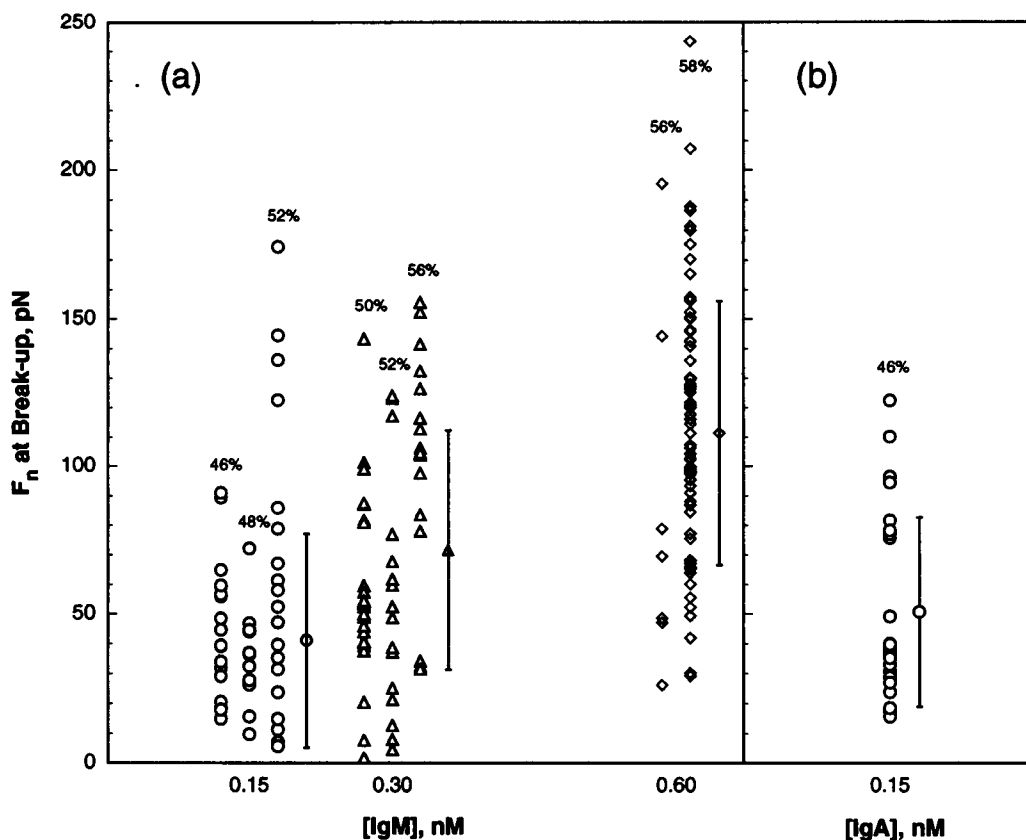
FIGURE 2 (a) Scatter plot of the normal force, F_n, at break-up at [IgM] = 0.15, 0.30, and 0.60 nM. Results obtained at different [sucrose] at the same [IgM] are shown in separate columns; the percentage sucrose is indicated at the top of each column. (b) Scatter plot of normal force, F_n, at break-up at [IgA] = 0.15 nM. Error bars show 1 SD from the mean for all points at each [antibody].

Data for the different buffered sucrose concentrations used at the same antibody concentration are shown as separate columns with the sucrose percentages indicated at the top. The mean and SD of the combined sucrose concentration data are shown to the right of each [IgM] column.

As previously found with the polyclonal antibody (Tha et al., 1986), there was considerable overlap in the range of F_n without any evidence of clustering at discrete values. The data for $\langle F_n \rangle$ at the different [IgM] and [sucrose] are shown in Table 1. If the data at different [sucrose] for a given [IgM]

TABLE 1 Poiseuille flow—constant slow acceleration: normal force at break-up versus [IgM]

[IgM] (nM)	[Sucrose] (%)	η, 25°C (mPa·s)	No. of doublets	$\langle F_n \rangle \pm$ SD (pN)	
0.15	46	8.52	18	45 ± 23[a]	
	48	10.2	12	36 ± 16[a,b]	50 ± 36[c]
	52	16.7	19	63 ± 50[b]	
0.30	50	12.7	23	58 ± 31[d]	
	52	16.7	16	55 ± 39[d,e]	70 ± 40[c]
	56	25.1	20	100 ± 38[e]	
0.60	56	16.7	7	87 ± 61[f]	111 ± 45[c]
	58	25.1	78	113 ± 43[f]	

[a, d] Not significantly different.
[b, c, e, f] $P < 0.05$.

are averaged together, the mean measured force increases significantly with increasing [IgM]. This could be interpreted as signifying an increase in the average number of antigen-antibody bonds, as it was for the polyclonal results (Tha et al., 1986; Tha and Goldsmith, 1988). Closer analysis, however, reveals that for [sucrose] = 52%, the values of $\langle F_n \rangle$ at 0.15 and 0.30 nM IgM (63 and 55 pN, respectively) are not significantly different. A similar result is found for [sucrose] = 56%, $\langle F_n \rangle$ at 0.30 and 0.60 nM IgM (100 and 87 pN, respectively). Furthermore, many of the average forces for different [sucrose] at the same [IgM] are significantly different. It seems, then, that in these experiments the increase in $\langle F_n \rangle$ seen in the graph is due mostly to increasing [sucrose] rather than to increasing [IgM]. Since an increase in [sucrose] corresponds to an increase in suspending medium viscosity, and in F_n, it is likely that high sucrose concentrations caused weakly bound doublets to break up before they could be observed, and doublets that would otherwise have escaped from the lower end of the tube unbroken to break up. Both of these mechanisms would tend to produce higher average forces. In the presence of such viscosity artifacts, it is not possible to observe the expected increase in $\langle F_n \rangle$ with increasing [IgM].

Six of the doublets in suspensions containing 0.15 and 0.30 nM IgM broke up at $F_n < 10$ pN (Fig. 2 a). These particles

either separated within the first 10 rotations or rotated for longer times in orbits having $C < 0.1$, in which case $\theta_1 \ll 90°$ and the angle factor in Eq. 7 $\ll 1$, throughout the orbit.

Similar measurements of the normal force of break-up carried out in 46% buffered sucrose containing 0.15 nM anti-blood group B IgA are shown in Fig. 2 b. The mean normal force of break-up for the IgA antibody was 51 ± 32 pN, not significantly different from that obtained at 0.15 nM IgM in 46% sucrose, 45 ± 23 pN.

The absence of evidence for clustering at discrete force values at any of the [IgM], in both the monoclonal and polyclonal antibody results, led us to examine the time dependence of break-up.

Poiseuille flow: halted rapid acceleration

These experiments, designed to test both the time and force dependence of doublet break-up at a constant shear rate, were all carried out in suspensions containing 52% sucrose to avoid possible viscosity effects. The suspensions were rapidly accelerated to reach steady velocities corresponding to maximum F_n from 10 to >200 pN. Of 280 doublets tracked in the microtube, 24 (9%) broke up during the acceleration phase, and a further 41 (15%) broke up during steady flow. With the exception of five doublets, break-up occurred within 30 s of the onset of steady flow. Of the remaining 215 doublets (76%), which did not break up before being lost at the lower end of the tube, 80% were tracked for >30 s.

Time distribution of break-ups

Since it is predicted that the average doublet time to break-up is force dependent (Bell, 1978; Evans et al., 1991a) and should decrease with increasing applied force, the time to break-up after the start of steady Poiseuille flow, t_P, was examined as a function of hydrodynamic force. Table 2 shows the average time to break-up, $\langle t_P \rangle$, for a high $(F_n \geq 70$ pN) and a low $(F_n < 70$ pN) range of forces at the two [IgM] used. It is evident that, in a given force range, the $\langle t_P \rangle$ for the two [IgM] were not significantly different, although there was a trend toward a shorter average time for the lower concentration of antibody. Surprisingly, antibody concentration has little effect on the times to break-up. Increasing the force range does, however, decrease $\langle t_P \rangle$, although the differences are still not statistically significant, even for the combined [IgM] data, where $\langle t_P \rangle$ at $F_n \geq 70$ pN is 40% lower than that at $F_n < 70$ pN.

TABLE 2 Poiseuille flow—halted rapid acceleration: average time to break-up after start of steady flow

Applied force (pN)	$\langle t_P \rangle \pm$ SD (s)		
	0.075 nM IgM	0.150 nM IgM	Combined data
$F_n < 70$	17.3 ± 14.5^a ($n = 5$)	19.4 ± 21.9^a ($n = 16$)	18.8 ± 20.1^b
$F_n \geq 70$	8.5 ± 6.2^c ($n = 6$)	12.6 ± 14.7^c ($n = 14$)	11.3 ± 12.7^b

[a, b, c] Not significantly different.
n, No. of doublets.

Since the values of $\langle t_P \rangle$ at the two IgM concentrations were not significantly different, the data were combined in the histogram of Fig. 3 to show the number distribution of doublet break-ups as a function of t_P at $F_n < 70$ and ≥ 70 pN. With increasing t_P, the ratio of doublets broken under low applied F_n to all the doublets broken up in the time range rose from 44% in the interval $0 < t_P < 5$ s, to 60% at $t_P \geq 15$ s. It appears that doublets exposed to high F_n tended to break up slightly faster than those exposed to low F_n.

Force distribution of break-ups

Since the forces to which doublets were exposed in steady flow were known, both for those that broke up and those that did not, the fraction of all doublets observed that broke up under a given applied normal force were computed. The results obtained in the two force ranges and at the two [IgM] are given in Table 3. Here, it is evident that [IgM] had an effect on the fraction of doublets that broke up: the fractions at 0.075 nM IgM are 1.7 and 1.5 times larger than those at 0.150 nM IgM in the low and high force range, respectively.

The distribution, over four force ranges, of the number of doublets that did and did not break up is shown in the histogram of Fig. 4 for data obtained at 0.150 nM IgM. It can be seen that the fraction of doublets that broke up increases slowly with increasing F_n: 8.5% of doublets broke up at $F_n < 30$ pN, whereas 30% broke up at $F_n \geq 90$ pN.
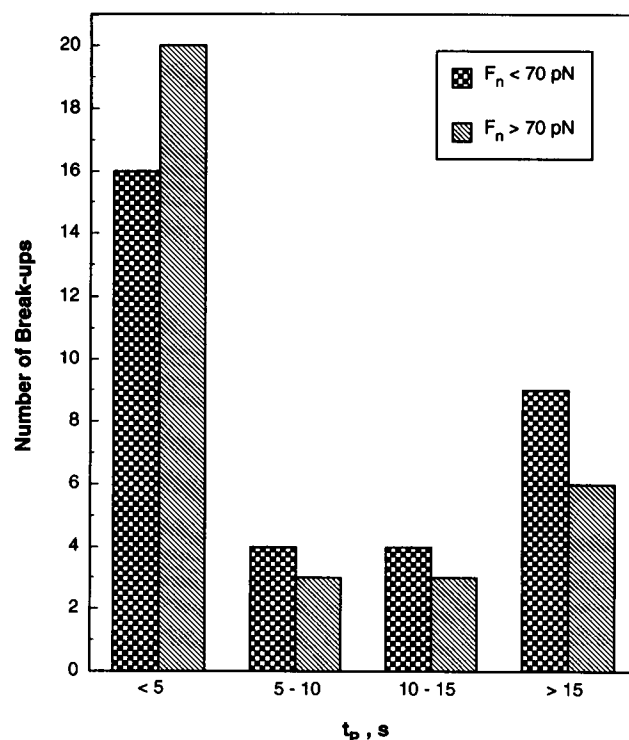

FIGURE 3 Histogram of the number of break-ups in Poiseuille flow as a function of the time to break up after the start of steady flow, t_P, divided into four ranges, for the high $(F_n \geq 70$ pN) and low $(F_n < 70$ pN) force ranges; data at 0.075 and 0.15 nM IgM are combined.

TABLE 3   Poiseuille flow—halted acceleration: fraction of doublets broken up in low and high force ranges

Applied force (pN)	Fraction of break-ups	
	0.075 nM IgM	0.150 nM IgM
$F_n < 70$	0.17 ($n = 30$)	0.10 ($n = 160$)
$F_n \geq 70$	0.40 ($n = 15$)	0.27 ($n = 51$)

n, No. of doublets.

Couette flow: immediate application of shear

The halted acceleration experiments were complicated by the relatively long acceleration period required to achieve the desired shear rate, 37% of all break-ups occurring during this time. Furthermore, the period of acceleration introduces uncertainty into the calculation of the time that a doublet spends under a given force, since in many cases the time spent in steady flow is comparable to the time spent in acceleration. For an unambiguous determination of the break-up time, the application of the desired shear stress should be instantaneous. The rheoscope's acceleration period of 60 ms to maximum shear rate allowed this ideal to be very closely approximated. The shear rates varied from 9 to 90 s^{-1}, encompassing a range of maximum applied normal force from 30 to >200 pN. Of the 340 doublets analyzed, 125 (37%) broke up before being lost to view, ~10 s after flow commenced.

Temporal distribution of break-ups

Distribution in times. The time to break-up in Couette flow, t_C, was determined for all doublets examined. The values of $\langle t_C \rangle$ obtained in the three force ranges $F_n < 70$ pN, $70 \leq F_n < 140$ pN, and $F_n \geq 140$ pN are given in Table 4. In computing these averages, only the data for break-ups within 10 rotations have been used, since only 9 (of 125) doublets broke up after this point, and many doublets not seen to break up were lost before this number of rotations had been completed. Furthermore, a standardized cutoff value is necessary for a proper comparison with the results of the simulation described below. As in Poiseuille flow, the values of $\langle t_C \rangle$ in a given force range were not significantly different at 0.075 and 0.150 nM [IgM], but in Couette flow the decrease in $\langle t_C \rangle$ with increasing F_n was significant at each [IgM]. For the combined data, $\langle t_C \rangle$ decreased by a factor of 1.6 in going from $F_n < 70$ pN to $70 < F_n < 140$ pN, and by a further 2.2 times in going to the highest force range. Most striking, however, were the much shorter break-up times in Couette flow, the values of $\langle t_C \rangle$ being 30 and 17% of those in Poiseuille flow at $F_n < 70$ pN and $F_n \geq 70$ pN, respectively.

The distribution of break-up times for the combined 0.075 and 0.150 nM data is illustrated in Fig. 5. With increasing force, there was a marked increase in the number of break-ups at the shortest t_C, followed by a sharp decrease in the succeeding seconds. In the force range $F_n < 70$ pN, the number of break-ups fluctuated between 2 and 5 over the 6
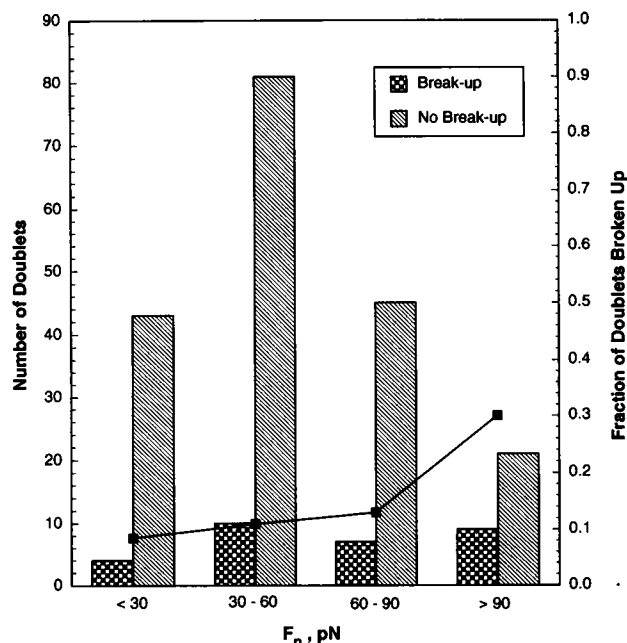

FIGURE 4   Histogram of the number of break-ups and no break-ups in Poiseuille flow as a function of F_n, divided into four ranges, at 0.15 nM IgM. The line shows the variation in the fraction of doublets broken up with increasing F_n.

TABLE 4   Couette flow—immediate application of shear: average time to break-up for doublets breaking within 10 rotations

Applied force (pN)	$\langle t_C \rangle \pm$ SD (s)		
	0.075 nM IgM	0.150 nM IgM	Combined data
$F_n < 70$	2.64 ± 1.80^a ($n = 10$)	2.39 ± 1.80^a ($n = 9$)	2.52 ± 1.66 $P < 0.02$
$70 \leq F_n < 140$	1.92 ± 1.67^b ($n = 16$)	1.40 ± 1.38^b ($n = 36$)	1.56 ± 1.49 $P < 0.01$
$F_n \geq 140$	-^{c}	0.70 ± 0.74 ($n = 43$)	0.70 ± 0.74

[a, b] Not significantly different.
n, No. of doublets.
[c] No data.

time ranges shown, and there was no significant dependence on time. In the two higher force ranges, however, there was a marked decrease in the number of break-ups with increasing time, from a maximum observed at the shortest t_C, during the first second. In the highest force range, the decrease continued, and all but one of the 47 doublets broke up within 5 s. In the intermediate force range, the number of break-ups fluctuated between 5 and 10 after the initial decrease. Beyond 10 s, only 3 break-ups were observed, in spite of the considerable number of doublets (62) that were observed for a longer period than this.

Distribution of rotations. As pointed out in the theoretical section, in shear flow, the applied force varies periodically, the doublets being subjected to tensile forces twice during each orbit. The number distribution of break-ups, plotted as a function of the number of rotations from the onset of shear, therefore yields information on the number of times the particles were exposed to a given force. Using the measured period of rotation, we computed the fraction of doublets
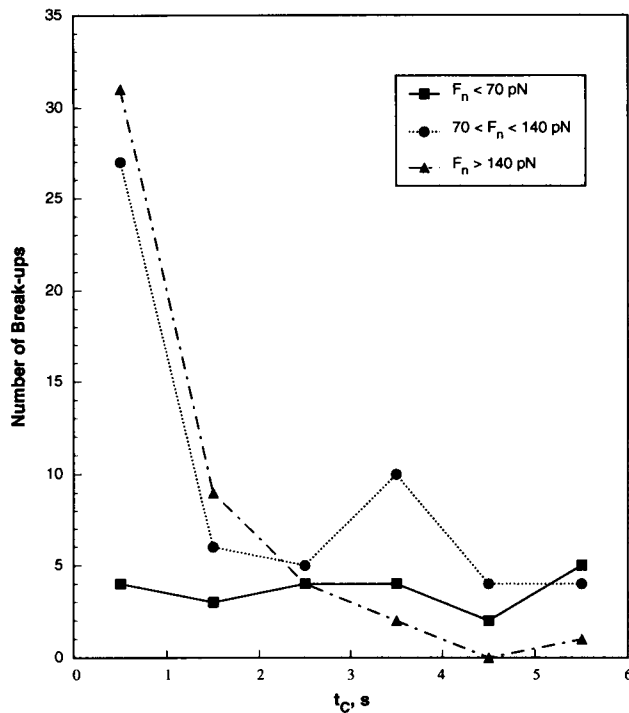
FIGURE 5   Plot of the number of break-ups in Couette flow as a function of time to break-up, t_C, divided into 1-s periods, for the high ($F_n \geq 140$ pN), intermediate ($70 \leq F_n < 140$ pN), and low ($F_n < 70$ pN) force ranges; data at 0.075 and 0.150 nM IgM are combined.
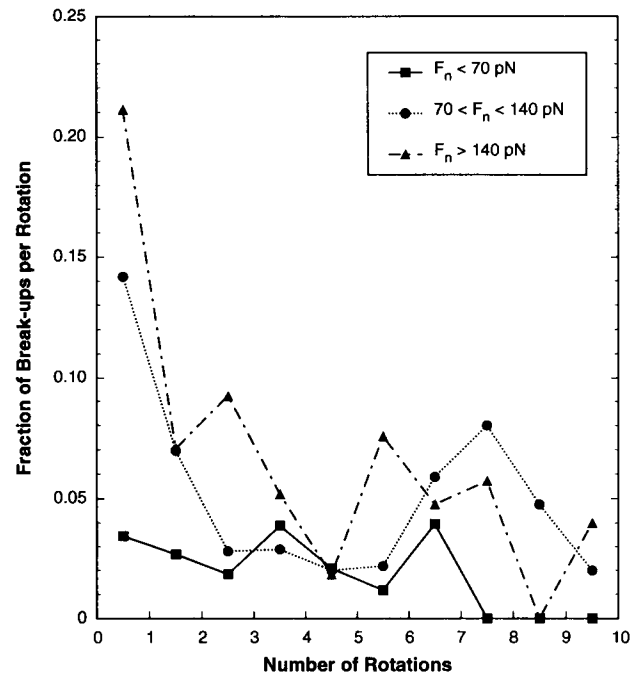
FIGURE 6   Plot of fraction doublets breaking up per rotation (the fraction of the total number of doublets observed in that rotation which broke up) during the first 10 rotations after the onset of shear, for the high ($F_n \geq 140$ pN), intermediate ($70 \leq F_n < 140$ pN), and low ($F_n < 70$ pN) force ranges; data at 0.075 and 0.150 nM IgM are combined.

that broke up *in a given rotation*, that is, the fraction of the total number of doublets observed in that rotation that broke up. Fig. 6 shows the fraction of break-ups per rotation for the first 10 rotations.

As expected from the data shown in Fig. 5, in the intermediate and high force ranges, most of the break-ups occurred within the first rotation. Thus, there was a significant decrease in the fraction of break-ups from the first to the second rotation, from 14 and 21% in the intermediate and highest force range, respectively, to 7%. This was followed by marked fluctuations over the next six rotations. In the lowest force range, the fraction of break-ups fluctuated between 1.5 and 4% in the first seven rotations, after which no more doublets broke up.

Force distribution of break-ups

The fractions of all doublets observed that broke up within 10 rotations in the high, intermediate, and low force ranges at the two IgM concentrations used are given in Table 5. As was the case in Poiseuille flow, the fraction of break-ups at both [IgM] increased with increasing applied force and the values at the low [IgM] were both 1.5 times those at the high [IgM] in the low and intermediate force ranges. It is evident, however, that in each force range, a considerably larger fraction of doublets broke up in the Couette flow experiments than in the halted acceleration experiments in Poiseuille flow (Table 3).

A more detailed analysis of the dependence of the proportion of break-ups on applied force is shown in Fig. 7 for

TABLE 5   Couette flow—immediate application of shear: fraction of doublets breaking up within 10 rotations

Applied force (pN)	Fraction of break-ups	
	0.075 nM IgM	0.150 nM IgM
$F_n < 70$	0.20	0.13
	($n = 49$)	($n = 67$)
$70 \leq F_n < 140$	0.52	0.35
	($n = 31$)	($n = 103$)
$F_n \geq 140$	-[a]	0.47
		($n = 90$)

n, No. of doublets.
[a] No data.

the data obtained at 0.150 nM IgM. The figure shows histograms of the number of doublets that broke up and did not break up, as well as a plot of the fraction of break-ups as a function of F_n in seven 30 pN-wide ranges. The fraction of break-ups increased most rapidly in the lower force ranges from 15% at $30 \leq F_n < 60$ pN to 43% at $90 \leq F_n < 120$ pN. At $F_n \geq 180$ pN, over 60% of doublets broke up.

DISCUSSION

Slow acceleration in Poiseuille flow

The results of the constant slow acceleration experiments using polyclonal and monoclonal antibodies show that, in both cases, (*a*) the normal forces at break-up at different concentrations of antibody exhibit considerable overlap and (*b*) there is no evidence of clustering at discrete normal force
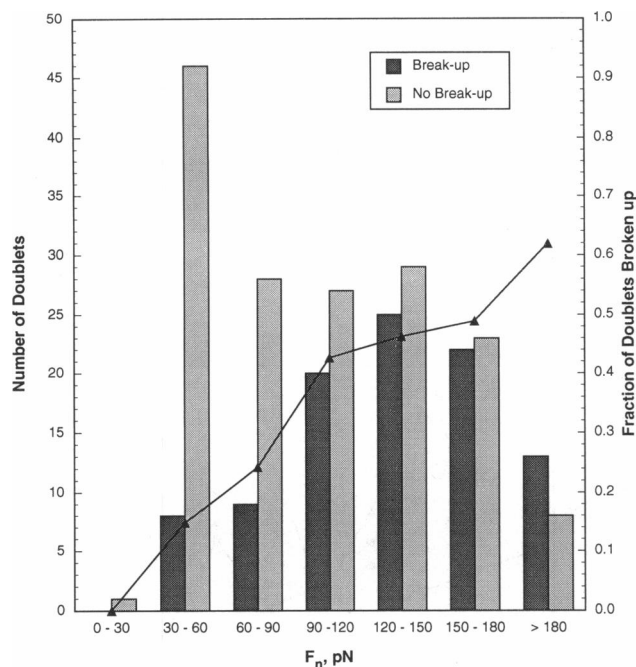
FIGURE 7   Histogram of the number of break-ups and no break-ups in Couette flow as a function of F_n, divided into seven ranges, at 0.150 nM IgM. The line shows the variation in the fraction of doublets broken up with increasing F_n.

values. The first similarity suggests that, as before, there is a distribution in the number of antibody-antigen bonds linking the observed doublets, producing a large scatter in force values. Bond formation is considered to be a Poisson process (Capo et al., 1982), and therefore a large scatter in the number of bonds, and hence F_n, at low bond number is to be expected. χ^2 goodness of fit and Poisson heterogeneity tests have been applied to determine the force required to break one bond. The data for polyclonal antiserum are consistent with a minimum force of 24 pN (Tha et al., 1986). The same tests on the 0.15 nM monoclonal antibody data yield a value of 20 pN. Although one would expect the average force at break-up to increase with increasing [antibody] (due to an increase in the number of cross-bridges), the increase in $\langle F_n \rangle$ observed with increasing monoclonal [antibody] is more plausibly explained by the increase in [sucrose] for the reasons mentioned in the Results (see Continuous Slow Acceleration).

The lack of clustering at discrete values of the F_n at break-up in the polyclonal experiments can be attributed to the presence of antibodies to different antigenic determinants of the same antigen in the polyclonal antiserum and to experimental error (about $\pm 10\%$). The presence of a unique molecule specific to a single determinant in the monoclonal preparations, however, should lead to clustering at force values corresponding to one bond, two bonds, three bonds, etc., since a force of 20 pN to break up one bond is considerably larger than the measurement error of about ± 2 pN at this value of F_n. The observed lack of clustering is, therefore, surprising. Furthermore, the above argument cannot account for the existence of six break-ups at $F_n < 10$ pN (Fig. 2 a),

forces much lower than the ostensible 20 pN required to break one bond, based on fitting the Poisson distribution. In any case, the results obtained in the halted rapid acceleration experiments in Poiseuille flow and those in the immediate shear application experiments in Couette flow strongly support the notion that break-up is a time-dependent, stochastic process.

The results obtained in slowly accelerating Poiseuille flow can then be accounted for by attributing a lifetime to the bonds that cross-link the doublets. By the time the doublet separates, the force at break-up will be higher than the value that would have been necessary had the particle been allowed to break up under a lower constant shear stress applied for the same time. Since there is a distribution in the times for a doublet to break up under a given force, it is expected that there will be a distribution in the extent of overestimation of the force at break-up, leading to an absence of clustering in the data. In the next section, we use a time-dependent and stochastic treatment of bond breakage, suggested by Evans et al. (1991a), and show that it can be used to model results such as those illustrated in Fig. 2. Before describing the model, however, it is appropriate to discuss similarities and differences between the results obtained in Poiseuille and Couette flow.

Time and force dependence of break-up

One observation, common to both Couette and Poiseuille flow, is the decrease in mean time to break-up, $\langle t_{C,P} \rangle$, with increasing maximum applied force. In Poiseuille flow, $\langle t_P \rangle$ in the high force range is 60% of that in the low force range. In Couette flow, the reduction is even greater, with $\langle t_C \rangle$ in the high force range being 28% of that in the low force range. The decrease can be ascribed to the force dependence of the average lifetime of the bonds that link the cells, using the stochastic model of break-up described below.

Another similarity in Couette and Poiseuille flow is the decrease in the fraction of break-ups with increasing antibody concentration at a given applied force, a fact that can be interpreted as an increase in the average number of bonds linking the cells of a doublet; the larger the number of bonds linking the cells, the less likely they are to break up. In view of this observation, the observed lack of significance between $\langle t_P \rangle$ and $\langle t_C \rangle$ at 0.075 and 0.150 nM IgM is all the more surprising. One explanation for this apparent contradiction is that the distribution of bonds in those doublets broken up by flow remains almost the same at different antibody concentrations. The forces applied by the flow, it might be argued, are capable of breaking up only doublets with a limited (and probably small) number of bonds, given the restricted time of observation. At low antibody concentration, these small numbers of bonds are more common than at high concentration, and hence the fraction of break-ups is larger; however, the difference in distribution of these small bond numbers at the two antibody concentrations would not change significantly enough to produce a noticeable change in $\langle t \rangle$.

The apparent paradox will be discussed further in the results of the Couette flow simulations below.

Although the variation of $\langle t \rangle$ with applied force is qualitatively the same in Couette and Poiseuille flow, the values of $\langle t_P \rangle$ are 3 and 5 times greater than the corresponding $\langle t_C \rangle$ in the low and intermediate F_n ranges, respectively. These differences are partly due to artifacts in the measurement of the tails of the break-up time distribution. In the rheoscope, doublets tended to be lost quickly (usually within 10 rotations), leading to a lack of data at long observation times. In halted, rapid acceleration, however, the short-time break-ups often occurred during the acceleration period of 5 to 15 s and were not included in the computation of $\langle t_P \rangle$. These differences aside, the very short (<1–5 s) break-up times frequently seen in Couette flow were much rarer in Poiseuille flow, even if allowance is made for the smaller number of particles in the latter experiments. Furthermore, the fractions of break-up in Couette flow are all ~ 1.3 times larger than the fractions in Poiseuille flow, which would suggest a larger number of bonds per cell in Poiseuille flow. A possible explanation for this difference is given below when the results of the simulation for the halted acceleration experiments are discussed.

Locus of failure

The question of locus of bond failure must also be addressed. Evans et al. (1991a), using a micropipette aspiration technique to measure the force of separation between a chemically fixed and unfixed red cell, showed that the forces deduced for short-time failure of 1–2 molecular attachments were nearly the same for a variety of agglutinins, between 10 and 20 pN. The molecular point attachments studied included a polyclonal antiserum to the blood group A antigen, a monoclonal IgA antibody (R10) to the integral membrane protein glycophorin A, and a lectin from the snail *Helix pomatia*. Similarly, in the present constant slow acceleration experiments, the average force at 0.15 nM IgA for 46% sucrose, 51 ± 32 pN, was not significantly different from that for the same concentration of IgM and sucrose, 45 ± 23 pN, despite the fact that these are different molecules specific to different antigenic determinants.

Furthermore, Evans et al. (1991a) showed, by means of microfluorometric tests, that labeled surface molecules were transferred from the surface of the unfixed to the fixed cell after separation of large areas of adhesive contact. These results show that the bond failed because the receptors were extracted from the membrane of the unfixed cell, and it was deduced that the rupture force represented a common process of molecular extraction from a hydrophobic bilayer core.

Can such receptor extraction occur when both cells are fixed? Microfluorometric tests using micropipette aspiration on chemically fixed cells (SSRC) (Tha, unpublished results) proved inconclusive, most probably because of leakage of fluorescent label into the interior of the cells. However, recent work by Xia et al. (manuscript submitted for publication) suggests that receptor extraction is possible, presumably from the lipid-linked antigenic sites. In these experiments, a suspension of 150-nm-diameter latex spheres coated with anti-blood group B antibody was incubated with a suspension of blood type B SSRC. After the latex spheres had coated the red cell surface, the suspension was sheared to detach the particles. It was found that the hydrodynamic size of the latex spheres, measured by photon correlation spectroscopy, had increased significantly after interaction with the SSRC. This implies that, as suggested by Evans et al., antigen molecules were extracted from the cell membrane during detachment of the latex spheres under shear.

Stochastic break-up model

A stochastic theory of doublet break-up has been suggested by Bell (1978) and Evans et al. (1991a) which should apply whether the mechanism of failure is bond breakage or antigen extraction. In this approach, which is based on the kinetic theory of the strength of solids, the free energy of a receptor-ligand bond, as a function of receptor-ligand displacement, has a minimum at an equilibrium distance, and increases as the separation distance, r, increases. The depth of this minimum is E_o (the free energy change on binding), and its "width" is r_o. If a force is applied to the bond, the minimum becomes shallower, and disappears completely when a "critical" value $f_c = E_o/r_o$ is reached. A force of this magnitude will result in almost instant bond failure. Bond break-up, however, is still possible at forces less than f_c. The equation relating the lifetime, t_b, to the force per bond, f, is predicted to have the form

$$t_b = t_o \exp(-c \cdot f) \tag{15}$$

where t_o and c are constants, particular to the bond, which may be determined empirically (Bell, 1978; Evans et al., 1991a). According to Bell (1978), $t_o = \tau_o \exp(E_o/kT_K)$, where τ_o is the reciprocal of the natural frequency of oscillation of atoms in solids ($\sim 10^{-13}$ s), T_K is the absolute temperature, and k is the Boltzmann constant. When $f \ll E_o/r_o$, $t_b \approx t_o$; however, as the applied force increases to the "critical" value ($f_c = E_o/r_o$), the average time required to break the bond decreases nonlinearly to a value on the order of τ_o. The other constant in Eq. 15, c, predicted (Bell, 1978) to be $\sim r_o/kT_K$, determines the extent of reduction in the energy minimum with applied force.

If, following Bell (1978), we make the identification $\kappa = 1/t_b$, where κ is the antigen-antibody bond reverse reaction rate constant, the probability of bond breakage, P_b, in a short time interval, Δt, has been shown to be (Hammer and Apte, 1992)

$$P_b = 1 - \exp(-\kappa \Delta t) = 1 - \exp\left[-\frac{\exp(c \cdot f)}{t_o} \Delta t\right]. \tag{16}$$

This equation predicts that there is a finite probability of bond breakage, even in the absence of an applied force. The doublets that broke up during measurement of SSRC size and orientation while the rheoscope was not rotating would seem

to be an example of this phenomenon. Similar break-ups were also occasionally observed in Poiseuille flow.

Computer simulation

In order to determine what the stochastic theory predicts for break-up in Couette and Poiseuille flow, a computer simulation of doublet break-up under shear was developed. In the model, t_o and c are parameters to be varied to fit the data collected in the Poiseuille and Couette flow experiments. The number of bonds holding the cells together, N_b, must also be provided since it is necessary for computation of f, the force per bond. We postulate that the force is divided equally among the bonds linking the cells. This is only an approximation, since bonds are distributed about the contact area, and they will no doubt experience unequal stresses, depending on their exact position. As long as the number of bonds is small, however, the approximation should be fairly good. Since, as mentioned previously, bond formation is thought to be ideally a Poisson process (Capo et al., 1982), specification of the average number of bonds, $\langle N_b \rangle$, is all that is required to characterize the distribution of bond numbers when fitting the experimental data.

For immediately sheared Couette flow simulations, the shear rate required to achieve a chosen maximum value of F_n was determined for a given orbit constant. For continuous slow and halted rapid acceleration from zero velocity in Poiseuille flow, $G(R)$ was determined from the elapsed time using the $dG(R)/dt$ corresponding to the simulated radial distance of the doublet center of rotation. In both cases, the period of rotation was found from the shear rate using Eq. 4. Each rotation was divided into N_s equal time steps of duration $\Delta t = T/N_s$; here N_s was chosen to be 900. The viscosity was taken to be 0.018 Pa·s, equal to that of 52% sucrose at 23.5°C.

The computer was programmed to begin a simulated break-up attempt by randomly choosing the number of bonds linking the members of the simulated doublet from a Poisson distribution with a preset average number of bonds, $\langle N_b \rangle$. The orbit constant for the doublet was randomly chosen from a sample of 40 experimental C values, a procedure that should reproduce the actual distribution of orbit constants in the Couette and Poiseuille flow experiments. In Poiseuille flow, the simulated radial distance was randomly chosen within the range $30 \leq R < 65$ μm. Simulation of shear-induced rotation was then initiated. For each time step, P_b was computed from Eq. 16 using the chosen values of c and t_o, and the force per bond was calculated with Eq. 7 for the current instantaneous values of ϕ, $\theta(\phi,C)$, G, and N_b. A random number between 0 and 1 was chosen from a uniform distribution for each bond remaining. If the number drawn for a bond was less than P_b, the number of bonds was reduced by one, and the force per bond acting on the remaining bonds was recalculated. It was assumed that no bonds formed over the course of the simulated experiment.

In Couette flow, the cycle of probability calculation and break-up testing was repeated, until the number of bonds was reduced to zero, or 30 s had elapsed, simulating the loss of doublets from the field of view. The fraction of break-ups per rotation, the $\langle t \rangle$, and the fraction of break-ups in the first 10 rotations were then computed for comparison with the experimental data. For halted, rapid acceleration in Poiseuille flow, calculations were repeated until break-up occurred or the preset shear corresponding to the desired maximum F_n was attained. The doublet was then treated using the algorithm for Couette flow. Particle rotation was simulated until break-up or loss at the simulated end of the microtube, 4 cm from the starting point of acceleration. The average time to break-up in halted flow was recorded along with the average fraction of doublets broken up in halted flow and during acceleration. In slowly accelerating Poiseuille flow, calculations were repeated until break-up occurred or the maximum shear attainable (corresponding to the maximum tracking velocity of the traveling microtube) was reached. The normal force at break-up was recorded for each particle simulated.

The bond parameters supplied to the simulation are t_o, c, and the average value of the Poisson distribution of the bonds linking the cells, $\langle N_b \rangle$. The simulated experimental variables supplied were the maximum normal force, $F_{n, max}$ and the number of simulated doublets, n. The bond parameters were varied under simulated experimental conditions resembling those in the rheoscope and traveling microtube experiments, in an attempt to achieve a match to the experimental data.

Couette flow

Simulated experiments in Couette flow were run using t_o from 5 to 400 s, c from 0 to 10^{12} N^{-1}, and $\langle N_b \rangle$ from one to 12 bonds. Simulated experiments were done with 50 or 100 doublets (approximating the numbers used in actual experiments). Each set of 50 or 100 was repeated five times, and the fraction of break-ups per rotation averaged at $F_n = 55$, 111, and 167 pN, corresponding to the average experimental values in the low, intermediate, and high force ranges, respectively.

The best fit to the Couette flow fraction of break-ups per rotation was determined by computing a χ^2 statistic for the first four rotations at each of the above F_n. The minimum χ^2 value occurred at $c = 1 \times 10^{11}$ N^{-1}, $t_o = 100$ s, and $\langle N_b \rangle = 4$ bonds. Fig. 8 a shows the fraction of break-ups at the three values of F_n with $\langle N_b \rangle = 4$ bonds. The general features of the real experiments shown in Fig. 6 are quite well reproduced. Thus, at the intermediate and high F_n, there is an initial high fraction of break-ups in the first rotation (13 and 23%, respectively, compared to the actual experimental values of 14 and 21% in Fig. 6), followed by a significant decrease in the second rotation (to 7 and 3%, respectively, as compared to 7 and 7% in Fig. 6), succeeded by marked fluctuations in the remaining rotations. At the lowest F_n, the fraction of break-ups fluctuated between 0 and 3%, compared to 0 and 4% in Fig. 6. Fig. 8 b shows the contributions to the fractions of break-ups at $F_n = 167$ pN of doublets having a fixed $N_b = 1$, 2, or 5

bonds. It is striking to note that 100% of all doublets cross-linked by one bond break up in the first rotation. For doublets cross-linked by two bonds virtually all of the doublets have broken up by the third rotation. For doublets cross-linked by five bonds, however, no break-ups are predicted before the third rotation.

The average times of break-up within 10 rotations were also computed at the three values of F_n and are given in Table 6 for $N_b = 1, 2$, and 5. As expected, there is a marked increase in $\langle t_C \rangle$ with increasing N_b and a marked decrease with in-

TABLE 6 Couette flow—simulated immediate application of shear: average times to break-up for doublets breaking within 10 rotations ($\eta = 0.018$ Pa·s)

$F_n{}^a$ (pN)		$\langle t_C \rangle \pm$ SD (s)	
	$N_b = 1$	$N_b = 2$	$N_b = 5$
55	2.32 ± 2.12	4.08 ± 2.15	$-^b$
111	0.022 ± 0.025	1.34 ± 1.13	1.98 ± 0.24
167	0.010 ± 0.003	0.11 ± 0.29	1.57 ± 0.47

^{a} Maximum value of normal force in each orbit.
^{b} No doublets broken within 10 rotations.
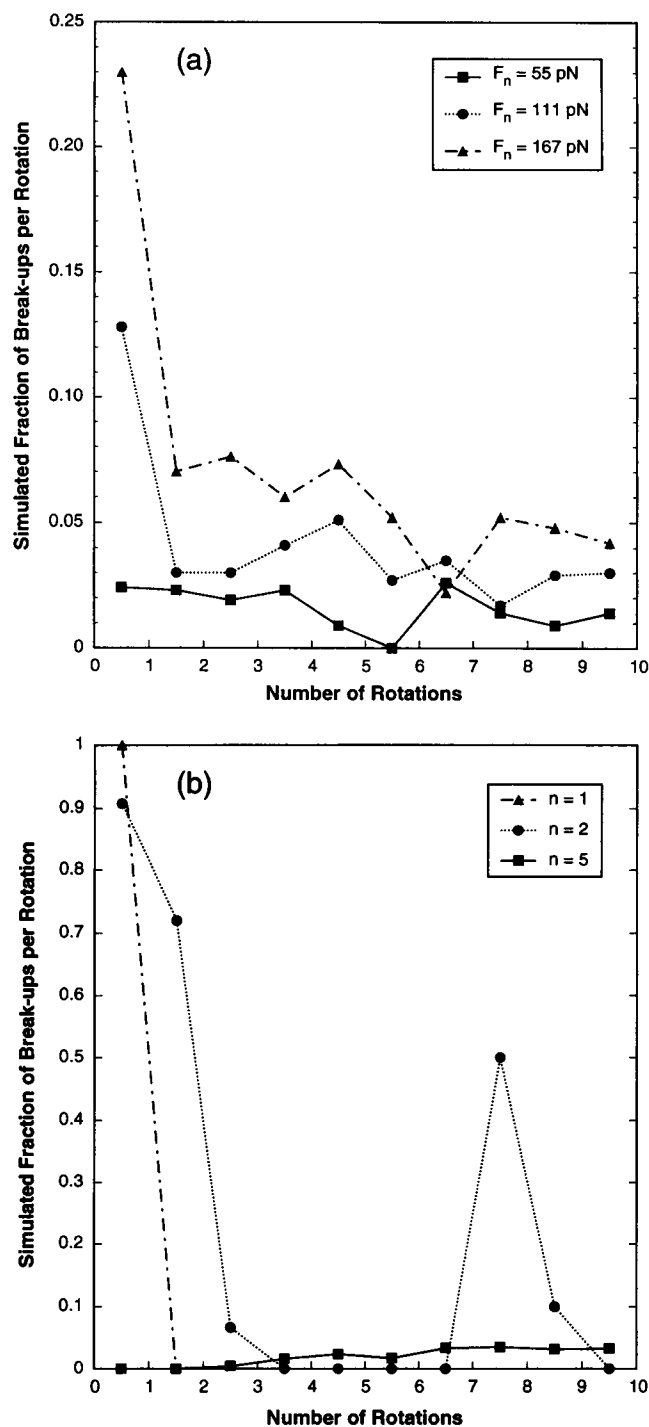
creasing F_n. It is found, however, that when there is a Poisson distribution of bonds, over a small range of c and t_o, $\langle t_C \rangle$ is roughly constant over a significant range of $\langle N_b \rangle$ (e.g., from 2 to 4 at $c = 1 \times 10^{11}$ N^{-1} and $t_o = 100$ s). The effect is shown in Table 7, which gives the values of $\langle t_C \rangle$ and the fraction of break-ups for the first 10 rotations for $\langle N_b \rangle = 2, 3$, and 4. Simulations were made for $n = 50$ and 100 doublets. While the fraction of break-ups is very similar at $n = 50$ and 100, decreasing with increasing $\langle N_b \rangle$, the values of $\langle t_C \rangle$ show no significant trend with increasing $\langle N_b \rangle$. This result of the simulation may explain the observed lack of dependence of $\langle t_C \rangle$ on antibody concentration.

A comparison of Table 7 with Tables 4 and 5 shows that the simulated data for $\langle N_b \rangle = 3$ and 4 appear to match fairly well the experimental fractions of break-up and to a lesser extent $\langle t_C \rangle$ at 0.075 and 0.150 nM, respectively, a result that deserves comment. That $\langle N_b \rangle$ does not double (i.e., from 2 to 4) with a doubling of the antibody concentration is not surprising since the relationship between bound and total antibody is complex and is known to be nonlinear.

The confidence with which the parameters t_o, c, and $\langle N_b \rangle$ were estimated deserves comment. Values of $c \le 2 \times 10^{10}$ N^{-1} were discarded, since the fraction of break-ups per rotation decreases with increasing force instead of increasing. This surprising behavior is due to the time history of force application. The time per rotation spent under normal or shear force in a single rotation, Δt (Eq. 9), decreases with increasing G. The force on the bond, however, increases with G. These two effects respectively lower and raise the probability of break-up, but whether P_b increases or decreases will depend on the value of c in Eq. 16. Consequently, the fraction of break-ups per rotation will also increase or decrease depending on c. By contrast, values of $c > 5 \times 10^{11}$ N^{-1} show very sharp decreases in the fraction of break-up after the first rotation, even for very high bond numbers. The chosen values of c and t_o are also unusual in having such a large range of N_b within which $\langle t \rangle$ is relatively constant. This explains why $\langle t_C \rangle$ does not change significantly with increasing [IgM].

FIGURE 8 (a) Plot of the fraction of doublets breaking up per rotation during the first 10 rotations after the onset of shear, for $F_n = 55$, 111, and 167 pN, produced by computer simulation of the shear-induced rotation of doublets in Couette flow. The best-fit parameters of the stochastic model (Eq. 15) were $t_o = 100$ s, $c = 1 \times 10^{11}$ N^{-1}, for $\langle N_b \rangle$ (mean value of the Poisson distribution in number of bonds) = 4. (b) Fraction of break-ups per rotation at $F_n = 167$ pN using the same t_o and c as in (a) for doublets having fixed values of $N_b = 1, 2$, and 5.

TABLE 7   Couette flow—simulated immediate application of shear: average times to break-up (η = 0.018 Pa·s)

$\langle N_b \rangle$	$F_n{}^a$ (pN)	n = 50 doublets		n = 100 doublets	
		$\langle t \rangle$ (s)	Fraction (%)	$\langle t \rangle$ (s)	Fraction (%)
2	55	3.51 ± 2.85	45	3.29 ± 2.88	44
	111	1.07 ± 1.34	72	1.12 ± 1.37	77
	167	0.33 ± 0.68	94	0.37 ± 0.71	90
3	55	3.74 ± 2.54	24	2.96 ± 2.18	23
	111	1.30 ± 1.43	52	0.91 ± 1.05	51
	167	0.38 ± 0.57	68	0.36 ± 0.17	71
4	55	3.15 ± 1.83	14	3.51 ± 2.62	15
	111	1.13 ± 1.18	28	1.27 ± 1.12	35
	167	0.47 ± 0.52	56	0.69 ± 0.77	54

^{a} Maximum value of normal force in each orbit.

The values of c and t_o found to match the Couette data can be used to predict E_o and r_o, the depth and range of the energy well in which the bond exists. Using the equations given above, E_o is found to be 0.9 eV (assuming $\tau_o = 10^{-13}$ s), and $r_o = 0.4$ nm. These are of the same order of magnitude as the values of Bell (1978) for a "representative antigen-antibody bond" of $E_o = 0.37$ eV and $r_o \sim 0.5$ nm. Using these values, the "critical force," f_c, required to completely eliminate energy minimum for one bond would be ~ 360 pN. For forces of this value, the bond lifetime should be $\sim 10^{-13}$ s. Obviously, almost instantaneous (i.e., <0.01 s) break-up will be seen at forces considerably less than this. By comparison, Bell (1978) predicts that the similar "critical force" for a covalent bond ($E_o = 3$ eV; $r_o = 0.14$ nm) should be 3400 pN. Thus the present antigen-antibody bond is ~ 10 times weaker than a covalent bond.

If indeed bonds are extracted from the membrane rather than ruptured, the range of the energy minimum, r_o, should be of the order of the thickness of one leaflet of the lipid bilayer (Bell, 1978), ~ 2 nm. Our best-fit value of 0.4 nm is significantly lower. Values of c corresponding to the leaflet thickness with reasonable values of t_o and N_b cannot match the data, resulting in a too rapid break-up of the doublets. Further work, using doublets of latex microspheres with covalently bound antigens, may shed light on this inconsistency.

Halted acceleration Poiseuille flow

Using t_o and c, found above, for Couette flow, the average times to break-up in halted acceleration Poiseuille flow were simulated for different bond numbers. Here it was found that the experimental results could not be reproduced using a simple Poisson distribution, reflecting the nonideal biological character of the suspensions used. For $\langle N_b \rangle = 4$ at $F_n = 38$ pN (the average of the experimental $F_n < 70$ pN), the simulated $\langle t_P \rangle = 50$ s, and at $F_n = 111$ pN (the average of the experimental $F_n \geq 70$ pN), the simulated $\langle t_P \rangle = 13$ s. These can be compared to the experimental values for 0.150 nM IgM of 19.4 s and 12.6 s for $F_n < 70$ pN and $F_n \geq 70$

pN, respectively. The fraction of break-ups in steady flow for $F_n = 38$ and 111 pN was 79% (plus 1% during acceleration) and 75% (plus 23% during acceleration), respectively, compared to experimental values of 10% and 27% ([IgM] = 0.150 nM; $F_n < 70$ pN and $F_n \geq 70$ pN, respectively). An attempt to achieve a better match of the data was made by varying c from 5×10^{10} to 5×10^{11} N^{-1} and t_o from 80 to 400 s. We found that the observed fractions of break-up and $\langle t_P \rangle$ could not be reproduced by any combination of c and t_o in the space searched for Poisson distributed N_b. The experimental results showed that almost invariably, if a doublet broke up, the break-up occurred either during acceleration or else in steady flow within the first third of the available tracking distance. In the simulation, however, at $c = 5 \times 10^{11}$ N^{-1} and t_o from 100 to 400 s, almost all doublets broke during acceleration, even for $\langle N_b \rangle > 12$, whereas at $c = 5 \times 10^{10}$ N^{-1} and t_o from 100 to 400 s, no doublets broke during acceleration, even for high force values, and the $\langle t \rangle$ values were far too high. For c values in between, either the fraction of doublets broken up was too high, or the $\langle t \rangle$ values were too long. Even when a distribution of force values that more accurately represented the spread of applied F_n was employed, the $\langle t \rangle$ remained too long. It would appear that the only way to match the data and still retain the theoretical Poisson distribution of bonds would be to use a bimodal distribution for the number of bonds linking doublets comprising two Poisson distributions: one representing the doublets linked by a large number bonds (say $\langle N_b \rangle > 16$), the other doublets having $\langle N_b \rangle \sim 4$.

One possible reason for a bimodal distribution in Poiseuille flow, and its apparent absence in Couette flow, lies in the different shear histories of the suspensions in Couette and Poiseuille flow prior to measurements of doublet break-up. In Couette flow, doublets were allowed to form by shearing the whole suspension at a uniform $G = 5.4$ s^{-1} for ~ 1 h and then suddenly increasing the shear rate to values as high as 90 s^{-1} for periods typically lasting 30 s. Such shearing is not conducive to the formation of doublets with multiple bonds. By contrast, in Poiseuille flow, most of the doublets likely formed in the 1.2-mm-diameter plastic tubing connecting the infusion reservoir with the 150-μm-diameter flow tube. The wall shear rates in the connecting tube are estimated to increase from 4×10^{-4} s^{-1} at the lowest flow rate used while searching for doublets, to 5×10^{-2} s^{-1} at maximum tracking velocity. At such low shear rates, the formation of multiple bonds is probable. At the same time, there would be a smaller population of doublets formed in the 1-cm entrance portion of the 150-μm microtube where the wall shear rate is ~ 0.2 s^{-1} while searching for doublets, which would have fewer cross-bridges. The effect of shear history on the measured force of separation had previously been reported in the micromanipulation experiments (Tha and Goldsmith, 1988).

Such a bimodal distribution in Poiseuille flow could also account for the observation that $\langle t_P \rangle$ is greater than $\langle t_C \rangle$. The simulation using only $\langle N_b \rangle = 4$ (that used in simulating Couette flow for 0.150 nM IgM) shows that at $F_n = $
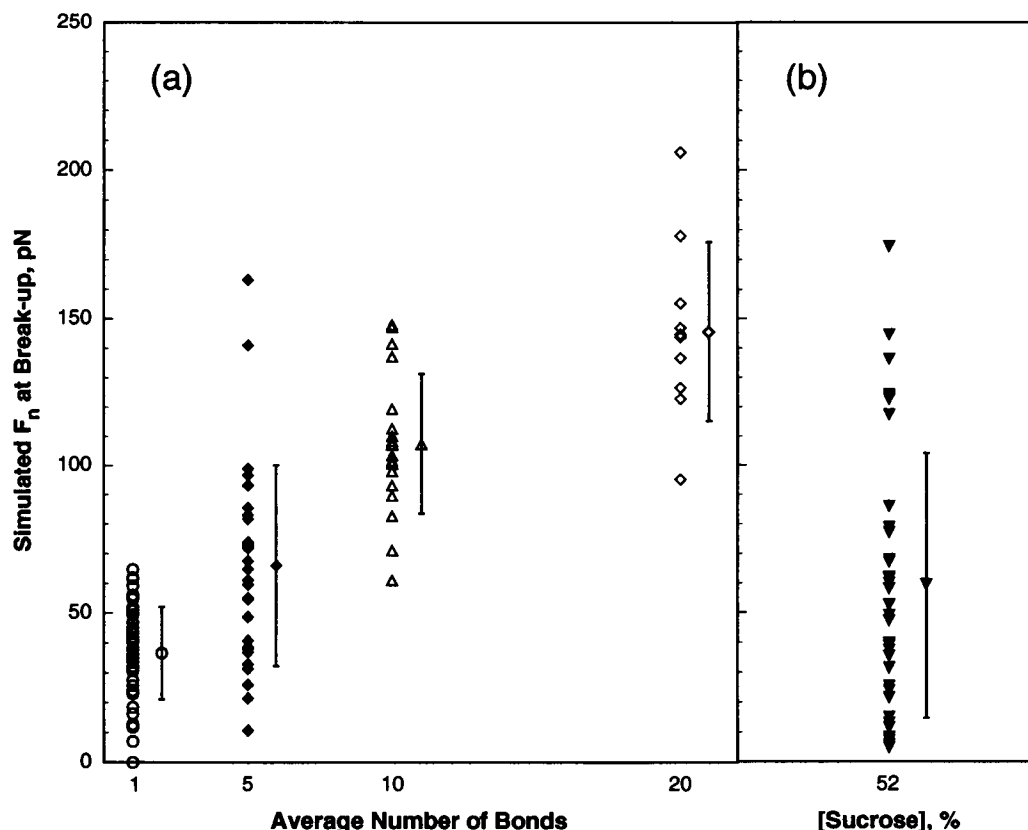
FIGURE 9 (a) Simulated scatter plot of F_n at break-up for constant slow acceleration in Poiseuille flow, as a function of the mean value, $\langle N_b \rangle$, of the Poisson distribution in number of bonds. The parameters of the stochastic model are the same as in the Couette flow simulation (Fig. 8). (b) Experimental scatter plot of F_n at break-up for the combined data at [IgM] = 0.15 and 0.30 nM for 52% sucrose.

111 pN, 88% of the doublets linked by one and two bonds break up during acceleration, yet it is just these doublets that break up in Couette flow at very short times. Their absence in Poiseuille flow will tend to produce longer average times. The doublets belonging to the population having high N_b do not contribute to the $\langle t_P \rangle$ since they do not break up in the available tracking distance, but they do contribute to the fraction of break-ups by increasing the fraction not broken up.

Constant slow acceleration in Poiseuille flow

Again, using t_o and c, found above, for Couette flow, the distribution of forces seen in continuous slow acceleration

of Poiseuille flow can be simulated for different bond numbers. Fig. 9 a shows such scatter plots for $\langle N_b \rangle$ = 1, 5, 10, and 20 bonds, and each series was carried out with 50 doublets. As the average number of bonds increases, the number of break-ups decreases from 41 to 10. The average force increases with increasing $\langle N_b \rangle$, and as shown in Table 8, all of the differences are statistically different. For comparison, the combined experimental force values at 0.15 and 0.30 nM IgM and 52% sucrose are shown in Fig. 9 b. Fig. 9 a demonstrates that, in order to match the experimental data at 52% sucrose in which there are significant numbers of break-ups at F_n < 20 pN as well as at F_n > 100 pN, one would again choose a bimodal distribution consisting of a $\langle N_b \rangle$ less than 5 and greater than 10.

TABLE 8 Poiseuille flow—simulated constant slow acceleration: normal force at break-up and number of bonds (η = 0.18 Pa·s)

$\langle N_b \rangle$[a]	No. of doublets in simulation	No. of break-ups	$F_n \pm$ SD (pN)
1	50	41	36.5 ± 15.4[b]
5	50	29	66.1 ± 33.9[b]
10	50	19	107.4 ± 23.8[b]
20	50	10	145.6 ± 30.4[b]

[a] Preset average number of bonds in a Poisson distribution.
[b] P < 0.001.

REFERENCES

Bell, G. I. 1978. Models for the specific adhesion of cells to cells. *Science (Washington DC)*. 200:618–627.

Bell, G. I., M. Dembo, and P. Bongrand. 1984. Competition between non-specific repulsion and specific bonding. *Biophys. J.* 45:1051–1064.

Berk, D., and E. Evans. 1991. Detachment of agglutinin-bonded red blood cells. III. Mechanical analysis for large contact areas. *Biophys. J.* 59:861–872.

Bevington, P. R. 1969. Data Reduction and Error Analysis for the Physical Sciences. McGraw-Hill, New York. 336 pp.

Bongrand, P., C. Capo, A. M. Benoliel, and R. Depieds. 1979. Evaluation of intercellular adhesion with a very simple technique. *J. Immunol. Methods.* 28:133–141.

Capo, C., F. Garrouste, A-M. Benoliel, P. Bongrand, A. Ryter, and G. I. Bell. 1982. Concanavalin-A-mediated thymocyte agglutination: a model for a quantitative study of cell adhesion. *J. Cell Sci.* 56:21–48.

Cozens-Roberts, C., D. A. Lauffenburger, and J. A. Quinn. 1990a. Receptor-mediated cell attachment and detachment kinetics. I. Probabilistic model and analysis. *Biophys. J.* 58:841–856.

Cozens-Roberts, C., J. A. Quinn, and D. A. Lauffenburger. 1990b. Receptor-mediated cell attachment and detachment kinetics. II. Experimental model studies with the radial-flow detachment assay. *Biophys. J.* 58:857–872.

Dembo, M., D. C. Torney, K. Saxman, and D. Hammer. 1988. The reaction limited kinetics of membrane-to-surface adhesion and detachment. *Proc. R. Soc. Lond. B. Biol. Sci.* 234:55–83.

Economidou, J., N. C. Hughes-Jones, and B. Gardner. 1967. Quantitative measurement concerning A and B antigen sites. *Vox Sang.* 12:321–328.

Evans, E. A. 1985. Detailed mechanics of membrane-membrane adhesion and separation. II. Discrete kinetically trapped molecular cross-bridges. *Biophys. J.* 48:175–183.

Evans, E., and A. Leung. 1984. Adhesivity and rigidity of erythrocyte membrane in relation to wheat germ agglutinin binding. *J. Cell Biol.* 98:1201–1208.

Evans, E., D. Berk, and A. Leung. 1991a. Detachment of agglutinin-bonded red blood cells. I. Forces to rupture molecular-point attachments. *Biophys. J.* 59:838–848.

Evans, E., D. Berk, A. Leung, and N. Mohandas. 1991b. Detachment of agglutinin-bonded red blood cells II. Mechanical energies to separate large contact areas. *Biophys. J.* 59:849–860.

Goldman, A. J., R. G. Cox, and H. Brenner. 1967. Slow viscous motion of a sphere parallel to a plane wall. I. Motion through a quiescent fluid. *Chem. Eng. Sci.* 22:637–652.

Goldsmith, H. L., and S. G. Mason. 1962. The flow of suspensions through tubes. I. Single spheres, rods and discs. *J. Colloid Sci.* 17:448–476.

Goldsmith, H. L., and S. G. Mason. 1967. The microrheology of dispersions. *In* Rheology: Theory and Applications. Vol. 4. F. R. Eirich, editor. Academic Press, Inc., New York. 85–250.

Hammer, D. A., and S. M. Apte. 1992. Simulation of cell rolling and adhesion on surfaces in shear flow: general results and analysis of selectin-mediated neutrophil adhesion. *Biophys. J.* 63:35–57.

Lawrence, M. B., and T. A. Springer. 1991. Leukocytes roll on a selectin at physiological flow rates: distinction from and prerequisite for adhesion through integrins. *Cell.* 65:859–874.

Sung, K-L. P., L. A. Sung, M. Crimmins, S. J. Burakoff, and S. Chien. 1986. Determination of junction avidity of cytolytic T cell and target cell. *Science (Washington DC).* 234:1405–1408.

Takamura, K., H. L. Goldsmith, and S. G. Mason. 1979. The microrheology of colloidal dispersions. IX. Effects of simple and polyelectrolytes on rotation of doublets of spheres. *J. Colloid Interface Sci.* 72:385–400.

Tha, S. P., and H. L. Goldsmith. 1986. Interaction forces between red cells agglutinated by antibody. I. Theoretical. *Biophys. J.* 50:1109–1116.

Tha, S. P., and H. L. Goldsmith. 1988. Interaction forces between red cells agglutinated by antibody. III. Micromanipulation. *Biophys. J.* 53:677–687.

Tha, S. P., J. Shuster, and H. L. Goldsmith. 1986. Interaction forces between red cells agglutinated by antibody. II. Measurement of hydrodynamic force of breakup. *Biophys. J.* 50:1117–1126.

Tözeren, A. 1990. Cell-cell, cell-substrate adhesion: theoretical and experimental considerations. *J. Biomech. Eng.* 112:311–318.

Tözeren, A., L. H. Mackie, M. B. Lawrence, P-Y. Chan, M. L. Dustin, and T. A. Springer. 1992. Micromanipulation of adhesion of phorbol 12-myristate-13-acetate-stimulated T lymphocytes to planar membranes containing intercellular adhesion molecule-1. *Biophys. J.* 63:247–258.

Vadas, E. B., H. L. Goldsmith, and S. G. Mason. 1973. The microrheology of colloidal dispersions. I. The microtube technique. *J. Colloid Interface Sci.* 43:630–648.

Wakiya, S. 1971. Slow motion in shear flow of a doublet of two spheres in contact. *J. Phys. Soc. Jpn.* 31:1581–1587 (errata [1972] 33:278).

Xia, Z., L. Woo, and T. G. M. van de Ven. 1989. Microrheological aspects of adhesion of *Escherichia coli* on glass. *Biorheology.* 26:359–375.